⌘ *Author's Choice*

THE JOURNAL OF BIOLOGICAL CHEMISTRY VOL. 283, NO. 22, pp. 15440–15450, May 30, 2008

Dual Specificity Phosphatases 18 and 21 Target to Opposing Sides of the Mitochondrial Inner Membrane*[S]

Received for publication, November 21, 2007, and in revised form, March 28, 2008 Published, JBC Papers in Press, April 2, 2008, DOI 10.1074/jbc.M709547200

Matthew J. Rardin[‡§], Sandra E. Wiley[‡], Anne N. Murphy[‡], David J. Pagliarini[¶1], and Jack E. Dixon[‡‖2]

From the [‡]Departments of Pharmacology, Cellular and Molecular Medicine, and Chemistry and Biochemistry, [§]Biomedical Sciences Graduate Program, and [‖]The Howard Hughes Medical Institute, University of California, San Diego, La Jolla, California 92093-0721 and the [¶]Department of Systems Biology, Harvard Medical School and Center for Human Genetic Research, Massachusetts General Hospital, Boston, Massachusetts 02114

Although large-scale approaches have identified numerous mitochondrial phosphoproteins, little is known about the mitochondrial kinases and phosphatases that regulate these phosphoproteins. Here, we identify two members of the atypical dual specificity phosphatases (DSP), DSP18 and DSP21, that are localized in mitochondria. Although DSP18 is widely expressed in several mammalian tissues, DSP21 is selectively expressed in the testes. We demonstrate that DSP18 and DSP21 are targeted to mitochondria by cryptic internal localization signals. Subfractionation of mitochondria demonstrated that DSP18 is located in the intermembrane space as a peripheral membrane protein of the inner membrane. In contrast, subfractionation of rat testis mitochondria revealed DSP21 is localized to the matrix as a peripheral membrane protein of the inner membrane. Moreover, we demonstrate that a previously reported substrate for DSP18, the stress-activated protein kinase, does not localize to mitochondria in several different tissues, making it an unlikely substrate for DSP18. Finally, we show that induction of apoptosis by treatment with staurosporine causes translocation of DSP18 from the intermembrane space into the cytosol similar to other apoptogenic factors such as cytochrome *c*. This work rigorously demonstrates the unique location of two highly similar DSPs on opposing sides of the mitochondrial inner membrane.

Regulation of reversible phosphorylation by protein kinases and phosphatases is one of the most common forms of post-translational modification and plays a vital role in numerous physiological processes including cell growth and differentiation, apoptosis, cell cycle, metabolism, sperm capacitation, and cytoskeletal organization (1–6). The primary work of Reed and co-workers (7) provides evidence that proteins in the mitochondria undergo reversible phosphorylation. Recent studies have suggested that reversible phosphorylation may participate to a greater extent than previously thought in regulating mitochondrial function (5, 6, 8–11). These findings are highlighted by the discovery that mutations in the mitochondrially localized kinase PINK1 (PTEN-induced kinase) are associated with a rare form of early onset Parkinson disease (12). In addition to kinases, a number of serine/threonine phosphatases are known to function in mitochondria, including the phosphatases for the E1 subunit of pyruvate dehydrogenase (7, 13) and the E1b subunit of the branched-chain α-keto acid dehydrogenase complex (14, 15).

In contrast to serine/threonine phosphatases, we recently identified the first dual specificity protein-tyrosine phosphatase (PTP),[3] PTPMT1, to exclusively localize to the inner membrane of mitochondria (16). PTPMT1 appears to play a critical role in pancreatic β-cell bioenergetics, since knockdown of PTPMT1 protein in INS-1 cells causes a significant increase in ATP production in response to low glucose. This in turn leads to an increase in glucose-stimulated insulin secretion (16).

There have been a limited number of other reports of PTP family members targeted to the mitochondrial outer membrane (OM) or intermembrane space (IMS). Shp-2, a predominately cytosolic non-receptor PTP can reside in the IMS. In addition, the mitogen-activated protein kinase phosphatase (MKP-1) and PTPD1 are suggested to localize to the cytosolic face of the mitochondrial OM in response to specific stimuli (17–19). MKP-1 is proposed to translocate to the OM antagonizing the pro-apoptotic effects of p38 MAPK on the anti-apoptotic factor Bcl-2 (17). PTPD1 is targeted to the mitochondrial OM via the protein kinase A anchoring protein (AKAP)-121 where it recruits and activates the tyrosine kinase Src (20). This

* This work was supported, in whole or in part, by National Institutes of Health Grant 18849 (to J. E. D.) and Pharmacology Training Grant NIH 2 T32 GM07752–25 (to M. J. R.). This work was also supported by the Walther Cancer Institute (to J. E. D.). The costs of publication of this article were defrayed in part by the payment of page charges. This article must therefore be hereby marked "*advertisement*" in accordance with 18 U.S.C. Section 1734 solely to indicate this fact.

⌘ *Author's Choice*—Final version full access.

[S] The on-line version of this article (available at http://www.jbc.org) contains supplemental Figs. 1–3.

[1] Current address: Dept. of Pharmacology, University of California, San Diego, La Jolla, CA 92093-0721.

[2] To whom correspondence should be addressed: Depts. of Pharmacology, Cellular and Molecular Medicine, and Chemistry and Biochemistry, University of California, San Diego, 9500 Gilman Dr., La Jolla, CA 92093-0721. Tel.: 858-822-0491; Fax: 858-822-5888; E-mail: jedixon@ucsd.edu.

[3] The abbreviations used are: PTP, protein-tyrosine phosphatase; OM, outer membrane; IM, inner membrane; IMS, intermembrane space; MP, mitoplast(s); SMP, submitochondrial particles; MAPK, mitogen-activated protein kinase; GST, glutathione *S*-transferase; BSA, bovine serum albumin; DAPI, 4′,6-diamidino-2-phenylindole; VDAC, voltage-dependent anion channel protein; Bis-Tris, 2-[bis(2-hydroxyethyl)amino]-2-(hydroxymethyl)propane-1,3-diol; EGFP, enhanced green fluorescent protein; ANT, adenine nucleotide transporter; SAPK/JNK, stress-activated protein kinase/Jun-N-terminal kinase; pNPP, *para*-nitrophenyl phosphate; SMAC, second mitochondria-derived activator of caspase; Hsp70, heat shock protein 70; DSP18 and DSP21, dual specificity phosphatases 18 and 21, respectively; IF, immunofluorescence; Mito, mitochondria; cyt c, cytochrome *c*.

signaling complex has been suggested to regulate ATP synthesis via modulation of mitochondrial metabolism (21).

Members of the atypical dual specificity phosphatases are poorly characterized enzymes no more than 250 amino acids in length (3). In addition, unlike classical DSPs, they lack Cdc25 homology domains (CH2) and kinase interaction motifs that mediate interaction with MAPKs (3, 22). The atypical DSPs contain the universal Cys-X_5-Arg (CX_5R) active site sequence motif characteristic of all PTPs and are distinguished by their *in vitro* ability to dephosphorylate both phosphotyrosine and phosphoserine/threonine residues (3, 22, 23). Two members of the atypical dual specificity phosphatases, DSP18 and DSP21, were originally identified via an EST data base search for tyrosine phosphatases (24). Concurrently, Wu *et al.* (25) cloned DSP18 from a cDNA library and showed it to be widely expressed in various tissues. DSP18 is a catalytically active phosphatase with a preference for phosphotyrosine over phosphoserine/threonine oligopeptides *in vitro* (24, 25). Recently, the crystal structure of human DSP18 was determined, revealing a unique C-terminal motif not seen in any known PTP structure (26). Comparison of the structure of DSP18 to the *Vaccinia* H1-related protein, VHR, reveals that the region critical for substrate recognition in VHR is absent in DSP18, suggesting a unique region for substrate recognition in DSP18 (26).

In the current study we demonstrate that transiently expressed DSP18 and DSP21 localize to the mitochondria. Furthermore, we demonstrate that endogenous DSP18 is localized to the IMS of rat kidney mitochondria where it peripherally associates with the IM. In contrast, DSP21 is targeted to the matrix compartment of mitochondria in testis tissue and, like DSP18, is peripherally associated with the IM. Our results reveal for the first time a DSP within the IMS compartment of mitochondria.

EXPERIMENTAL PROCEDURES

Cloning and Expression Constructs—The complete open reading frames of DSP14 (NP_008957), DSP24 (NP_076930), DSP18 (NP_776106) (Invitrogen), and DSP21 (ATCC-9898164) (27) were amplified by PCR from plasmids containing full-length cDNAs and cloned into pEGFP-N1, N2, or C1 (Clontech). DSP18 and DSP21 truncations were generated by PCR and ligated into pEGFP-N1.

Vectors for the expression of recombinant C-terminal His-tagged constructs were made using the pET21a vector (Stratagene). Murine forms of DSP18 and DSP21 were inserted into pET21a at 5′-NdeI and 3′-XhoI in-frame with the C-terminal His_6 tag. Vectors for expression of recombinant N-terminal GST-tagged protein were made using the pGEX-4T1 vector (GE Healthcare). DSP18 was inserted into pGEX4T1 at 5′-EcoRI and 3′-XhoI with a stop codon. Mutations were generated using site-directed mutagenesis. All constructs were verified by sequencing.

Protein Expression and Purification—Bacterially expressed recombinant DSP18-His_6 and DSP21-His_6 were expressed in BL21 (DE3) CodonPlus RIL cells (Stratagene) and purified using Ni^{2+}-agarose affinity resin (Qiagen) as described previously (28). Recombinant DSP18-His_6 and DSP21-His_6 were purified using Ni^{2+}-agarose affinity resin followed by separation over a Superdex 200 column (Amersham Biosciences).

Bacterially expressed recombinant GST-DSP18 was expressed in BL21 (DE3) CodonPlus RIL cells (Stratagene) and purified using glutathione-agarose affinity resin (Sigma) as described previously (29). Recombinant GST-DSP18 was further purified by gel filtration chromatography using a Superdex 200 column and stored at −80 °C in 10% glycerol, 2 mM EDTA, and 2 mM dithiothreitol.

Cell Culture, Transfection, Immunocytochemistry, and Materials—COS-7 cells were maintained at 37 °C at 5% CO_2 in Dulbecco's modified Eagle's medium (Invitrogen) containing 10% fetal bovine serum and 50 units/ml each penicillin and streptomycin. Transient transfections were performed using FuGENE 6 reagent (Roche Applied Science) according to the manufacturer's protocol. For immunocytochemistry, cells were incubated with 100 nM MitoTracker Red (Invitrogen) for 20 min before fixation with 3.7% formaldehyde and were then permeabilized in phosphate-buffered saline containing 0.1% Tween 20, 0.3% Triton X-100, and 6% BSA. Cells were incubated with anti-DSP18 serum at 1:1000 or anti-DSP21 at 1:100 in phosphate-buffered saline containing 0.1% Tween 20 and 6% BSA and Alexa Fluor 488 goat anti-rabbit-conjugated secondary antibody (Molecular Probes) at 1:500. Nuclei were stained with 300 nM DAPI (Molecular Probes) for 1 min before viewing. Fluorescence imaging was performed using a light microscope (DMR; Leica) with a PL APO 63× 1.32 NA oil objective (Leica) at room temperature, and images were captured with a CCD camera (C4742–95; Hamamatsu) using OpenLab 4.0.1 software (Improvision). The following antibodies were purchased: voltage-dependent anion channel protein (VDAC; Calbiochem #529536), second mitochondria-derived activator of caspase (SMAC)/DIABLO (Calbiochem #567365), calreticulin (Calbiochem #208910), cytochrome *c* (BD Biosciences #556433), NDUFB6 (Mitosciences #MS108), stress-activated protein kinase/Jun-N-terminal kinase (SAPK/JNK; Cell Signaling #9258), phospho-SAPK/JNK (Cell Signaling #9255), heat shock protein 70 (Hsp70; ABR #MA3028), enhanced green fluorescent protein (EGFP; BD Clontech #8371).

Generation of DSP18 and DSP21 Polyclonal Antibodies—Full-length recombinant GST-DSP18 (murine) or DSP21-His_6 (murine) was used to generate polyclonal anti-sera in rabbits (Cocalico). IgG was purified from serum using Prosep A (Millipore) chromatography according to manufacturer's protocol.

SAPK Activation Assay—Cells were washed once in phosphate-buffered saline buffer then treated with 40 mJ/cm^2 of ultraviolet light in a UV Stratalinker 2400 (Stratagene). After irradiation, growth medium was added, and cells were further incubated for 30 min.

Phosphatase Assays—Phosphatase assays were carried out in 50 μl of assay buffer containing 50 mM Bis-Tris, 25 mM Tris, and 2 mM dithiothreitol at pH 6 for 10 min at 30 °C. *para*-Nitrophenyl phosphate (pNPP) assays were performed as described previously (30).

Purification of Rat Kidney and Testis Mitochondria—Mitochondria were purified as described (31–33) with minor modifications. Fresh rat kidneys or testes were harvested and placed in ice-cold MSHE+BSA buffer (210 mM mannitol, 70 mM

sucrose, 5 mM HEPES, pH 7.4, with KOH, 2 mM EGTA, 0.5% fatty acid free BSA, and EDTA-free Complete protease inhibitor mixture (Roche Applied Science)). The renal capsule was removed, and kidneys were minced then washed 3 times in 150 mM NaCl and 3 times in MSHE+BSA buffer. Kidneys were disrupted with 10–15 strokes and testes 8–10 strokes of a tight fitting Potter-Elvehjem tissue homogenizer. Homogenate was centrifuged for 10 min at 600 × *g* to remove unbroken cells and nuclei. The pellet was re-homogenized and spun at 600 × *g*. Supernatants were combined and spun at 15,000 × *g* for 10 min to pellet mitochondria. Pellets were washed two times in MSHE+BSA followed by one wash in BSA-free MSHE buffer. Mitochondria were resuspended in 1–2 ml of MSHE and layered over a gradient of 35% histodenz (Sigma), 17.5% histodenz, and 6% Percoll (Sigma) that was centrifuged at 45,500 × *g* for 45 min at 4 °C. Mitochondria were collected from the 17.5–35% interface, centrifuged at 15,000 × *g* for 15 min, and resuspended in a small volume of MSHE buffer.

Immunogold Electron Microscopy—Rat kidney was perfused with 4% paraformaldehyde (PFA) in 0.1 M phosphate buffer and further immersion-fixed overnight in 4% PFA in phosphate buffer. Samples were rinsed with 0.15% glycine in 0.1 M phosphate buffer, pelleted in 10% gelatin in phosphate buffer, and cryoprotected by infusion with 2.3 M sucrose, phosphate buffer overnight at 4 °C. Tissue blocks (1 mm^3) were mounted onto specimen holders and snap-frozen in liquid nitrogen. Ultrathin cryosections (70–90 nm) were cut at −100 °C on a Leica Ultracut UCT with EM FCS cryoattachment using a Diatome diamond knife, picked up with a 1:1 mixture of 2.3 M sucrose and 2% methyl cellulose (15 cp) as described (34), and transferred onto Formvar- and carbon-coated copper grids. Immunolabeling was performed by slight modifications of the "Tokuyasu technique" (35) using anti-DSP18 at 1:2 followed by 10-nm gold-conjugated goat anti-rabbit IgG (GE Healthcare) at 1:25. Grids were viewed and photographed using a JEOL 1200EX II transmission electron microscope (JEOL, Peabody, MA).

Mitochondrial Subfractionation—Separation of inner and outer mitochondrial membranes was performed as described previously (16) with minor modifications. Gradient-purified mitochondria were resuspended in hypotonic solution (10 mM KCl, 2 mM HEPES, pH 7.2) at 5–8 mg/ml on ice for 20 min with gentle agitation. One-third volume of hypertonic solution (1.8 mM sucrose, 2 mM ATP, 2 mM $MgSO_4$, 2 mM HEPES, pH 7.2) was then added and allowed to incubate for an additional 5 min. Mitochondria were then sonicated with a probe for 15 s at 3 amps and layered on a step gradient containing 0.76, 1, and 1.32 M sucrose. Gradients were spun at 75,000 × *g* for 3 h at 4 °C. The IMS-soluble fraction was collected from the uppermost supernatant. The OM fraction was collected from the 0.76 and 1 M sucrose interface, washed with MSHE, and pelleted by centrifugation at 120,000 × *g*. Mitoplasts (MP) were collected from the pellet, washed with MSHE, and pelleted by centrifugation at 15,000 × *g*.

Submitochondrial particles (SMP) were generated from MP as described previously (36). MP were sonicated 3 × 2 min on ice with 1-min intervals. The solution was spun at 15,000 × *g* to remove intact MP, and the resulting supernatant was spun at 120,000 × *g* for 45 min at 4 °C to pellet SMP. The soluble matrix fraction was collected from the supernatant. SMP were washed once and resuspended in MSHE.

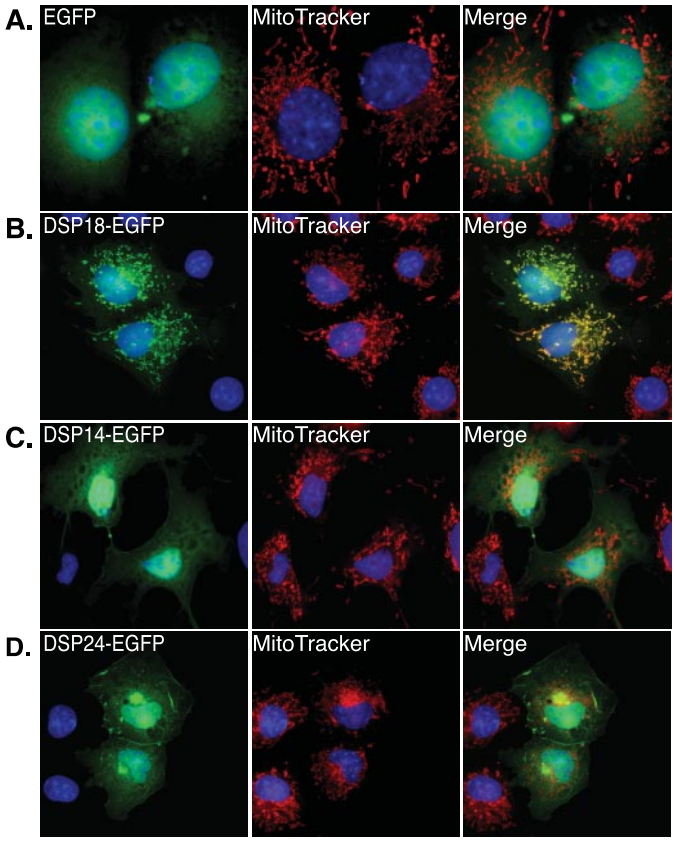

FIGURE 1. **Immunofluorescent analysis of predicted mitochondrial PTPs.** Fluorescent images of COS-7 cells transiently transfected for 24 h with constructs encoding EGFP only (*A*) or C-terminally EGFP tagged DSP18 (*B*), DSP14 (*C*), or DSP24 (*D*). Additionally, cells were stained with the mitochondrial marker, MitoTracker Red, and the nuclear marker, DAPI (*blue*). Co-localization is represented in the merged images in *yellow*.

Cytochrome c Translocation Assay—Assays for translocation of cytochrome *c* were performed as described previously (37). Briefly, apoptosis was induced in COS-7 cells by the addition of 500 nM staurosporine (Sigma) 2 h before fixation. Slides were prepared as described above and assessed visually using fluorescence microscopy.

RESULTS

Immunofluorescence Screen for Subcellular Localization of PTPs—Many of the ~107 PTPs are not well studied, especially the large number of atypical DSPs (3). As part of a larger effort to uncover the subcellular localizations of PTPs, we initially cloned full-length open reading frames of several genes into a vector encoding a C-terminal EGFP. We then transiently transfected COS-7 cells and analyzed subcellular localization via immunofluorescence (IF). Interestingly, of the PTPs we initially examined, only DSP18-EGFP redirected the predominantly cytosolic and nuclear EGFP to mitochondria, where it co-localized with the mitochondrial marker MitoTracker Red (Fig. 1*A* and data not shown). Mutation of the catalytic cysteine to serine showed no change in the ability of DSP18 to target to mitochondria (data not shown). In contrast, DSP14-EGFP and DSP24-EGFP did not show distinct subcellular localizations and did not co-localize with MitoTracker Red (Fig. 1, *C* and *D*).

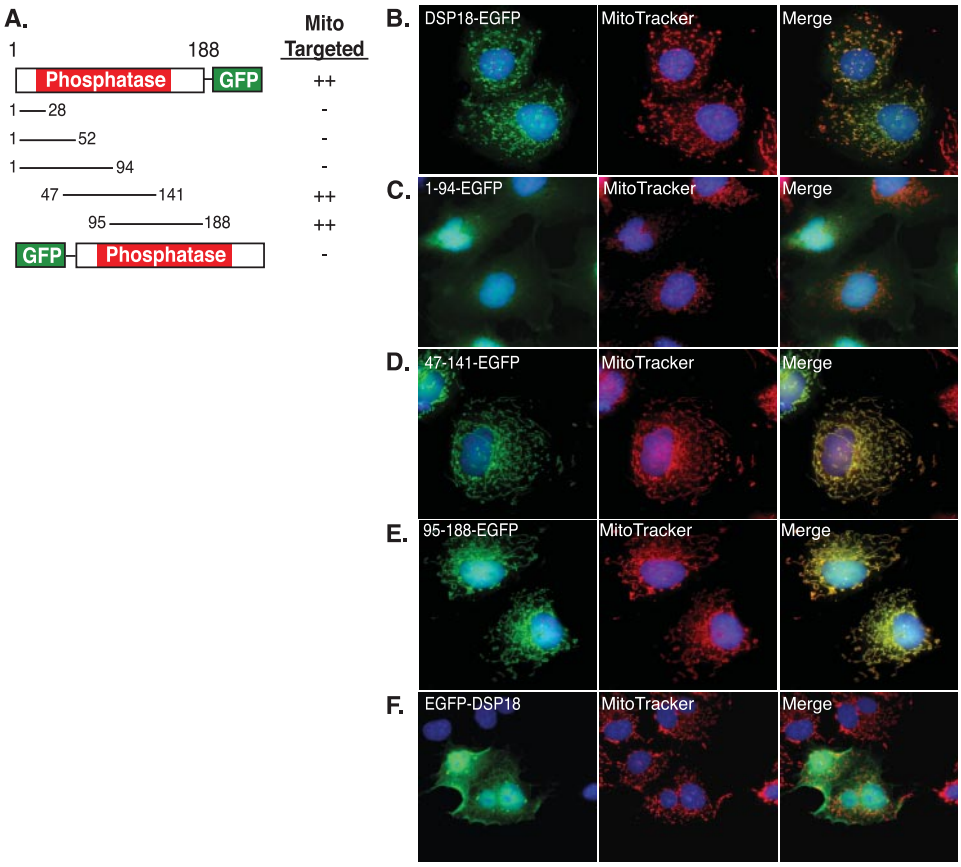

FIGURE 2. **An internal signal sequence directs DSP18 to mitochondria.** *A*, schematic of DSP18 truncations used to assess targeting of EGFP to mitochondria. COS-7 cells transiently expressing C-terminal EGFP-tagged DSP18 (*B*), 1–94-EGFP (*C*), 47–141-EGFP (*D*), 95–188-EGFP (*E*), and N-terminal EGFP-tagged DSP18. Fluorescent images were taken 24 h post-transfection after co-labeling with MitoTracker Red and DAPI (*blue*). Co-localization is represented in the merged images in *yellow*.

DSP18 Orthologs and Homologs—DSP18 is a class I cysteine-based PTP and falls into the atypical DSP subgroup, which currently contains 19 phosphatases (3, 25). We performed PSI-BLAST data base searches using the murine form of DSP18 and found that it is a highly conserved protein among vertebrates, with a potential ortholog in *Drosophila* (supplemental Fig. 1*A*). The DSP18 orthologs contain the active site consensus sequence (H/V)CX_5R(S/T) found in both classical and atypical DSPs but lack the MAPK interacting CH2 domain and kinase interaction motifs found in classical DSPs (supplemental Fig. 1*B*) (22).

DSP18 Has an Internal Mitochondrial Localization Signal—The discovery that DSP18-EGFP localizes to mitochondria led us to explore its targeting sequence. We generated several truncated constructs of DSP18 fused to the N terminus of EGFP (Fig. 2*A*) and transiently transfected these constructs into COS-7 cells. Although localization to the mitochondria is often encoded by the N terminus, the first 94 residues of DSP18 were unable to redirect EGFP from the cytosol and nucleus to mitochondria as compared with wild type DSP18 (Fig. 2, *B* and *C*). However, constructs containing amino acids 47–141 and 95–188 of DSP18 targeted EGFP to the mitochondria as indicated by colocalization with MitoTracker Red (Fig. 2, *D* and *E*). Furthermore, the placement of EGFP at the N terminus of DSP18 blocked localization of DSP18 to the mitochondria (Fig. 2*F*), suggesting that N-terminal epitope tags impede import into the mitochondria. The expression of DSP18 constructs was confirmed by immunoblotting with an anti-EGFP antibody (supplemental Fig. 2). Collectively these findings suggest an internal region of DSP18 from amino acid 95 to 141 is necessary for localization to mitochondria and that import requires an unconstrained N terminus.

Detection of Endogenous DSP18—To verify our overexpression studies, we examined the localization of endogenous DSP18. We generated a DSP18-specific, polyclonal antibody against full-length recombinant protein. The anti-DSP18 antibody did not cross-react with the highly similar protein DSP21 (Fig. 3*A*). IF analysis of endogenous DSP18 in COS-7 cells probed with the anti-DSP18 antibody exhibited mitochondrial localization (Fig. 3*B*). Cells probed with pre-immune serum (Fig. 3*C*) or cells stained with antibody blocked with recombinant GST-DSP18 showed no mitochondrial localization (Fig. 3*D*). Similar staining patterns were observed in HEK 293 cells and HeLa cells (data not shown). To biochemically confirm the IF results, we isolated highly purified mitochondria from homogenized rat kidneys by differential centrifugation followed by histodenz gradient purification. Immunoblot analysis demonstrated that endogenous DSP18 was highly enriched in the mitochondrial fraction along with the mitochondrial protein marker SMAC, whereas the endoplasmic reticulum protein marker calreticulin was removed during histodenz gradient purification (Fig. 3*E*).

To investigate the location of DSP18 at a higher resolution, we performed immunogold labeling of DSP18 of ultrathin cryosections from rat kidney tissue and COS-7 cells transiently expressing DSP18-EGFP (Fig. 3*F*, *panels 2* and *3*, respectively) and analyzed them by electron microscopy. Gold particles were found predominantly within mitochondria, suggesting DSP18 is localized to either the matrix, IM, or IMS, possibly the intracristal spaces (Fig. 3*F*). These results indicate that endogenous DSP18 is enriched in mitochondria and traffics to one of the interior compartments of the organelle.

Endogenous DSP18 Is an IMS Protein That Peripherally Associates with the Inner Mitochondrial Membrane—After identification of DSP18 as a mitochondrial protein, we sought to rigorously define its location within mitochondria. Rat kidney mitochondria were purified on a histodenz gradient as previously shown (Fig. 3*E*) and separated into the following fractions (Fig. 4*A*): OM, IMS (soluble material between the IM and OM),

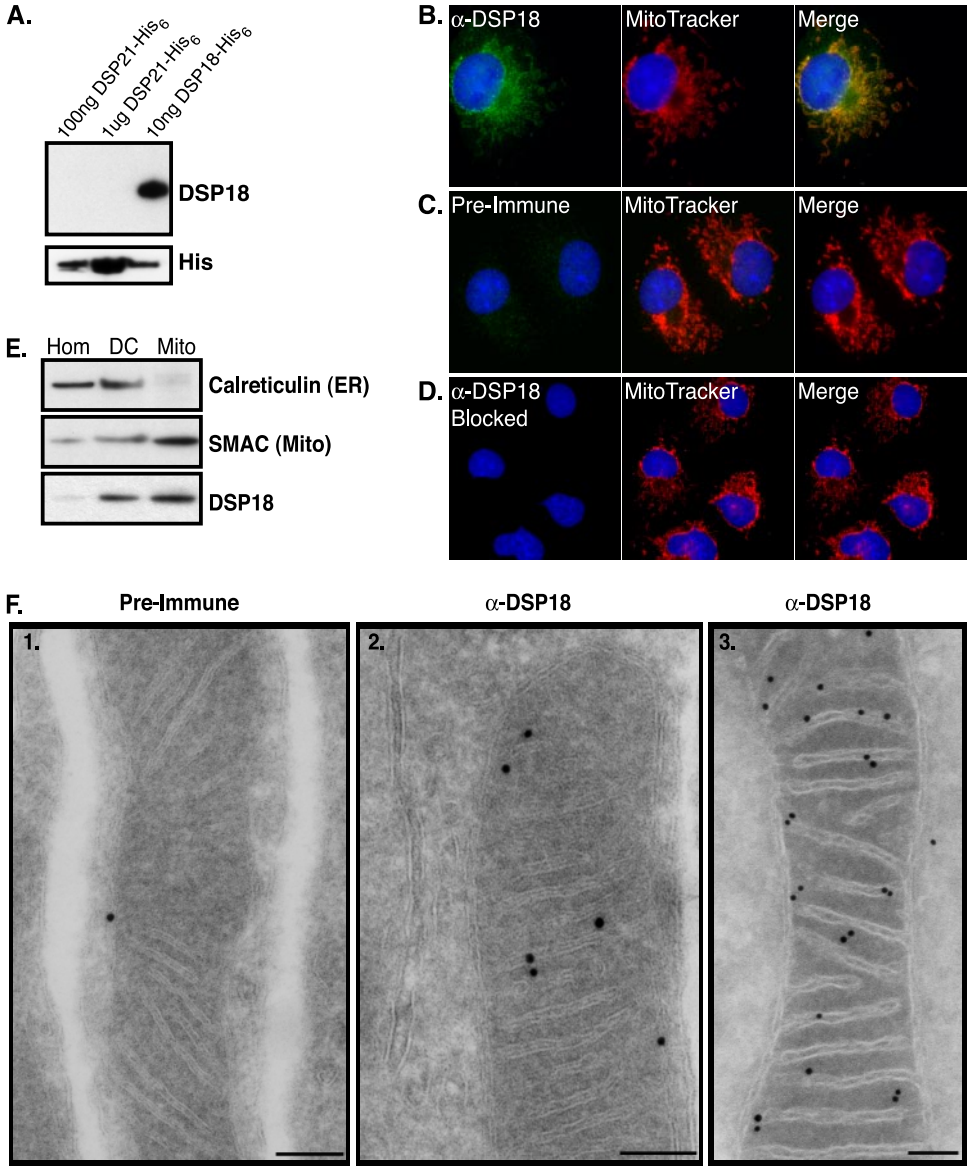

FIGURE 3. **Detection of endogenous DSP18.** *A*, for raising polyclonal antibody, recombinant DSP18-His_6 and DSP21-His_6 was purified from bacteria, separated by SDS-PAGE, and immunoblotted with protein A-purified anti-DSP18. Blots were stripped and reprobed with an anti-His antibody. Fluorescent images were taken of COS-7 cells probed with anti-DSP18 (*B*) and pre-immune serum (*C*), or anti-DSP18 was blocked with recombinant GST-DSP18 (*D*). *B–D*, cells were stained with MitoTracker Red and DAPI before visualization. Co-localization is represented in the merged images in *yellow*. *Bars*, 10 μm. *E*, 20 μg of rat kidney homogenate (*HOM*), differential centrifugation purified mitochondria (*DC*), and histodenz gradient-purified whole Mito were separated by SDS-PAGE and immunoblotted with anti-calreticulin (endoplasmic reticulum marker), anti-SMAC (mitochondrial marker), and anti-DSP18 antibodies. *F*, immunogold EM labeling of rat kidney sections (*1* and *2*) and COS-7 cells transiently expressing DSP18-EGFP (*3*). Sections were probed with Pre-Immune serum (*1*) or α-DSP18 antibody (*1* and *3*) and labeled with 10-nm gold-conjugated anti-rabbit secondary antibodies. *Bar*, 100 nm.

submitochondrial particles partially depleted of OM, mitoplasts (MP-intact IM and matrix), and soluble matrix. These fractions were blotted with antibodies against known marker proteins (Fig. 4*B*) for demonstration of purity. The VDAC, an OM marker, is enriched at contact sites between the outer and inner membranes and is, therefore, typically detected in both OM and MP/SMP fractions when using the swell/shrink separation method used here (16). DSP18 was enriched in the inner membrane-containing SMP and MP fractions (Fig. 4*B*), similar to PTPMT1, a known integral membrane protein located on the matrix side of the IM (16). A trace amount of DSP18 was also seen in the soluble matrix (*SM*) fraction (Fig. 4*B*).

Compartments within the mitochondria can have vastly different protein environments and, therefore, play differing roles in signaling events. Because of the location of DSP18 on the IM, we sought to determine whether DSP18 was located on the IMS or the matrix side of the IM. MP and SMP were treated with the proteolytic enzyme trypsin to cleave exposed proteins (Fig. 4*C*). In MPs treated with trypsin, DSP18 showed a decrease in signal over time in contrast to the matrix protein PTPMT1. However, DSP18 showed no loss of signal from SMP treated with trypsin, suggesting that DSP18 is attached to the IM facing the IMS compartment. The Complex I protein NDUFB6, which is buried within the IM, was used as a loading control.

To evaluate the strength of association of DSP18 to the IM, we washed either MP or pre-swollen whole mitochondria with high salt, an alkaline wash, pH 11.5, or control buffer. The whole mitochondria were pre-swollen to expose the outer surface of the inner membrane. DSP18 remained bound to the membrane after treatment with high salt but was subsequently released during the alkaline wash (Fig. 4*D*). Conversely, the tightly associated integral membrane protein PTPMT1 was not released by either treatment. Collectively, these results suggest that DSP18 is a mitochondrial IMS protein, which is peripherally associated with the IM predominantly along the cristae.

DSP21 Is a Highly Similar DSP That Is Also Targeted to Mitochondria via an Internal Mitochondrial Localization Signal—Using DSP18 as an index protein, we searched for other highly similar phosphatases that localize to mitochondria. Based on high sequence identity or similarity (69.3 and 80.4%, respectively), we identified a 21.5-kDa protein, DSP21, as a potential candidate for being targeted to mitochondria (Fig. 5*A*). To determine DSP21 subcellular localization, we transiently expressed a DSP21-EGFP fusion protein in COS-7 cells. Interestingly, DSP21-EGFP also showed mitochondrial localization when co-stained with MitoTracker Red (Fig. 5*B*). To verify our overexpression data, we generated a polyclonal

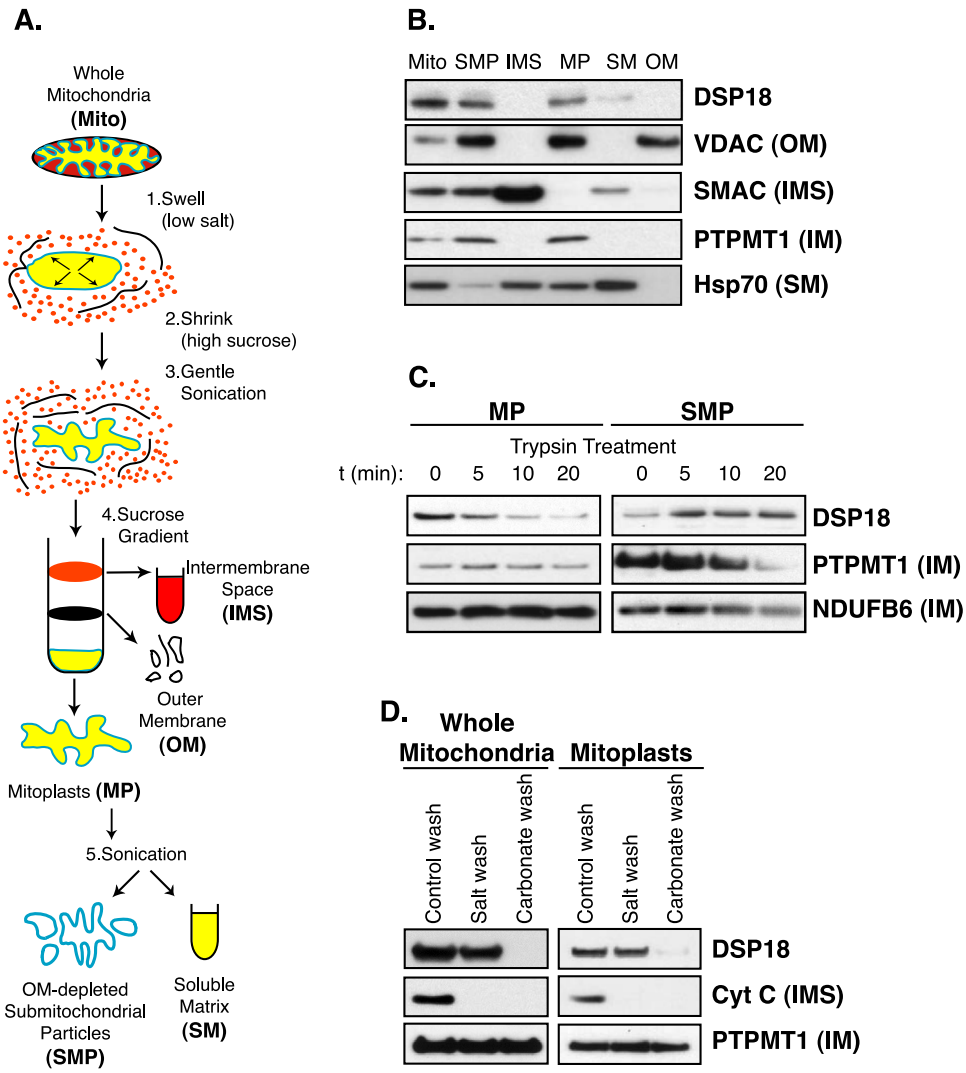

FIGURE 4. **DSP18 is associated with the inner mitochondrial membrane facing the intermembrane space.** *A*, diagram of mitochondrial subfractionation as described under "Experimental Procedures." *B*, 20 μg of each submitochondrial fraction (Fig. 4*A*) were separated by SDS-PAGE and immunoblotted with markers for OM (anti-VDAC), IMS (anti-SMAC), IM (anti-PTPMT1), and soluble matrix (*SM*; anti-Hsp70 – heat shock protein 70). *C*, 200 μg of MP and SMP were treated with 2.5 μg of trypsin in 100 μl of buffer for the indicated amounts of time. Samples were pelleted, washed, separated by SDS-PAGE, and immunoblotted with anti-DSP18 and anti-PTPMT1. The Complex 1 subunit NDUFB6 was not susceptible to trypsin digestion and was used as a loading control. *D*, 100 μg of osmotically swollen whole mitochondria and MP were washed with either control buffer, high salt (200 mM KCl, 2 mM HEPES, pH 7.2), or high pH (0.1 M Na_2CO_3, pH 11.5) buffer, repelleted, washed, and separated out by SDS-PAGE. Immunoblots were probed with antibodies against DSP18, cyt c, and PTPMT1.

To expand on our IF results, we analyzed DSP21 expression in different tissues at the mRNA level by reverse transcription-PCR as well as at the protein level by Western blot. Unlike DSP18, which is expressed in several different tissues, DSP21 protein appeared highly expressed only in testis tissue (data not shown). Although DSP18 mRNA was present in testes, we were unable to detect any protein expression of DSP18 in testis tissue (data not shown). We isolated highly purified mitochondria from rat testis homogenate by differential centrifugation followed by histodenz gradient purification. Western blot analysis demonstrated that DSP21 was highly enriched in the mitochondrial fraction along with the mitochondrial marker VDAC; however, the endoplasmic reticulum marker, calreticulin, was removed after gradient purification (Fig. 5*F*). In total, these data indicate that DSP21 is targeted to the mitochondria via an internal mitochondrial localization signal similar to DSP18, suggesting a common mechanism of import; however, these phosphatases vary in their tissue-selective expression.

DSP21 Is Localized to the Matrix and Peripherally Associates with the Mitochondrial Inner Membrane—To determine whether DSP21 is localized to the same compartment as DSP18, we sought to thoroughly define its location within rat testis mitochondria using the previously described fractionation method (Fig. 4*A*). The mitochondrial OM marker VDAC and the IM marker adenine nucleotide transporter (ANT) are both found at OM/IM contact sites; therefore, they can be found in both membrane fractions. The observation that DSP21 was enriched in both the SMP and MP fractions but not the OM suggests that DSP21 is localized to the IM (Fig. 6*A*). We examined its orientation on the IM using MP and SMP fractions treated with trypsin over time. MP treated with trypsin showed no loss of signal for DSP21 as assessed by Western blot (Fig. 6*B*). In contrast, trypsin-treated SMP fractions showed a rapid decrease in signal for DSP21 similar to that seen by the IM marker ANT. The electron transport chain Complex I subunit NDUFB6 was used as a loading control. Interestingly, these data suggest DSP21 is associated with the IM, but in contrast to DSP18, DSP21 is found facing the matrix compartment. As well, we treated SMP with either a buffer control, a high salt solution to

antibody against full-length recombinant DSP21 and labeled cells with anti-DSP21 antibody (Fig. 5*C*). IF analysis of endogenous DSP21 showed mitochondrial localization and co-labeled with MitoTracker Red. However, no mitochondrial localization was observed in cells stained with pre-immune serum or serum blocked with recombinant DSP21-His_6 (data not shown). The high degree of sequence similarity to DSP18 led us to investigate whether DSP21 also contained an internal mitochondrial localization signal. We generated several constructs containing truncations of DSP21 fused to EGFP and transiently transfected these constructs into COS-7 cells (Fig. 5*E*). Similar to DSP18, DSP21 is targeted to the mitochondria via an internal localization signal. Constructs containing amino acids 43–128 were both necessary and sufficient to redirect EGFP to the mitochondrion (Fig. 5, *D* and *E*).

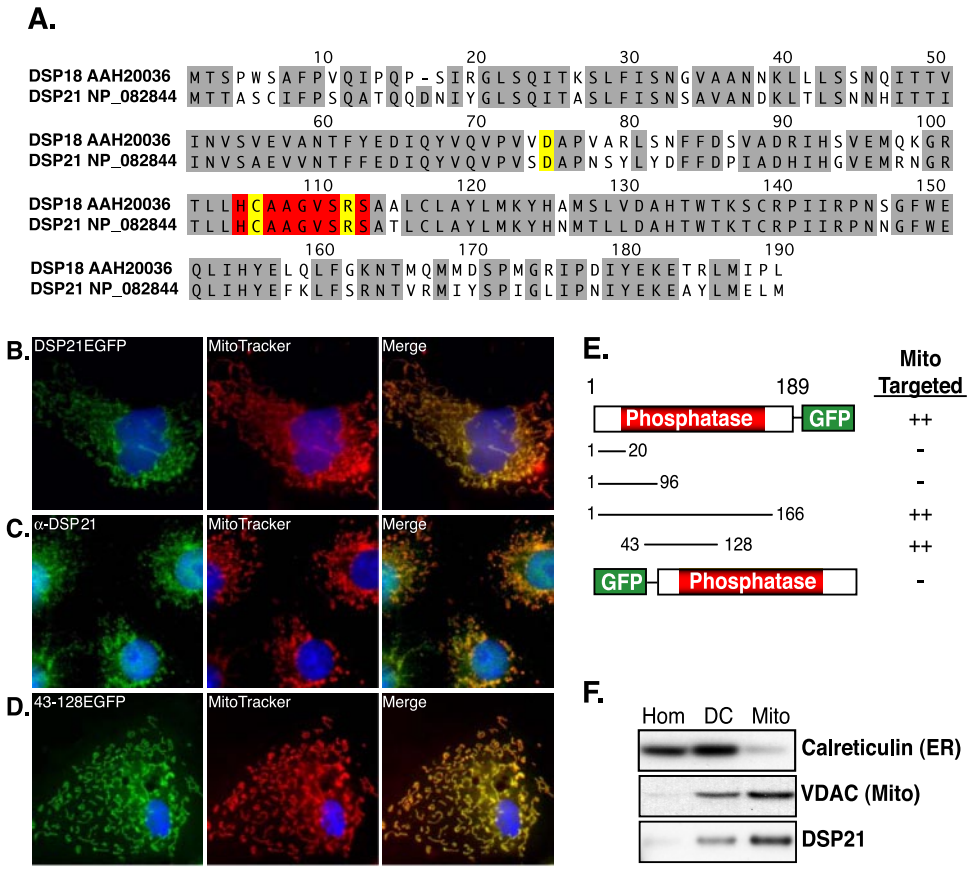

FIGURE 5. **DSP21 is a highly similar phosphatase to DSP18 localized to mitochondria.** *A*, sequence alignment of DSP18 and DSP21, with identities highlighted in *gray*, and the amino acids of the catalytic triad (*D*, *C*, *R*) highlighted in *yellow*. The active site residues (PTP-loop; CX_5R) are highlighted in *red*. GenBank™ accession numbers are listed next to the sequence. *B*, COS-7 cells transiently expressing C-terminal EGFP-tagged DSP21. *C*, fluorescent images were taken of COS-7 cells probed with anti-DSP21. *D*, COS-7 cells transiently expressing amino acids 43–128 of DSP21 with a C-terminal EGFP tag. *B–D*, cells were stained with MitoTracker Red and DAPI before visualization. Co-localization is represented in the merged images in *yellow*. *E*, schematic of DSP21 truncations used to assess targeting of EGFP to mitochondria. *F*, 20 μg of rat testis homogenate (*HOM*), differential centrifugation purified mitochondria (*DC*), and histodenz gradient purified whole Mito were separated by SDS-PAGE and immunoblotted with anti-calreticulin (endoplasmic reticulum marker), anti-VDAC (mitochondrial marker), and anti-DSP21 antibodies.

remove loosely associated proteins, or an alkaline wash to remove peripheral membrane proteins. Analogous to DSP18, DSP21 remained membrane-associated after the buffer control and high salt washes; however, SMP treated with the alkaline wash released DSP21 from the membrane as assessed by immunoblots using anti-DSP21 antibodies (Fig. 6*C*). In contrast, the ANT, an integral membrane protein of the IM, was not removed during the alkaline wash. This indicates that DSP21, like DSP18, is a peripheral membrane protein, and collectively these data suggest that DSP21 is localized to mitochondria in testis tissue where it peripherally associates with the IM within the matrix compartment.

Phosphatase Activity of DSP18 and DSP21—To demonstrate that DSP18 and DSP21 are catalytically active, the murine forms of DSP18 and DSP21 were expressed in bacteria, purified to homogeneity (data not shown), and assayed for phosphatase activity. Kinetic analysis of DSP18-His_6 and DSP21-His_6 was carried out using pNPP as a substrate. DSP18 and DSP21 had K_m values of 0.46 and 0.92 mM and k_{cat}/K_m values of 848 and 91.5 $s^{-1}\,M^{-1}$, respectively. Thus, DSP18 appears to be modestly more active than DSP21 against pNPP. DSP18 and DSP21 hydrolyze pNPP more efficiently than the DSPs MKP-3/rVH6 and PTPMT1 but not as efficiently as *Vaccinia* H1-related protein (VHR; Table 1) (38–41). Mutation of the catalytic active site cysteine to serine abolished phosphatase activity of both DSP18 and DSP21 (supplemental Fig. 3). These results demonstrate that DSP18 and DSP21 are catalytically active phosphatases having kinetic constants consistent with other members of the DSP family of phosphatases.

Currently there are several DSPs that have been reported to dephosphorylate MAPK (22). A recent report (42) describes DSP18 as a MAPK phosphatase with the ability to dephosphorylate the p54 SAPK/JNK using an overexpression system in HEK-293 cells. Because we have shown that DSP18 resides in the mitochondria, we thought it was important to investigate whether endogenous SAPK/JNK is localized to mitochondria where it could act as a substrate for DSP18. Because mitochondria can have different protein compositions in different tissues, we isolated mitochondria from kidney, liver, and testis. Rat tissue was isolated and separated into the following fractions: homogenate, post-nuclear supernatant, Mito (histodenz gradient-purified mitochondria), and post-mitochondrial supernatant. Equal amounts of each fraction were separated by SDS/PAGE and analyzed by immunoblotting with antibodies against SAPK/JNK, the mitochondrial marker Hsp70, and DSP18. SAPK/JNK was detected in the homogenate (*Homo*) and post-nuclear supernatant (*PNS*) and post-mitochondrial supernatant (*PMS*) fractions but not in the Mito fractions as compared with Hsp70 and DSP18 (Fig. 7*A*). The high sequence similarity between DSP18 and DSP21 led us to examine whether SAPK/JNK could possibly be found in mitochondria isolated from rat testes. Similar to the kidney fractions, SAPK/JNK was not detected in mitochondria isolated from testes (Fig. 7*B*). Moreover, SAPK/JNK was not detected in mitochondria from liver tissue, which does not express DSP18 or DSP21 (Fig. 7*C*).

To determine whether activation of SAPK/JNK was required for translocation to mitochondria, we treated HEK-293A cells with 40 mJ/cm^2 of ultraviolet (UV) light, a known activator of the SAPK/JNK pathway (43). After UV treatment, HEK-293A cells were homogenized, and crude Mito were isolated using differential centrifugation. Activation of SAPK/JNK was assessed by immunoblotting against the phosphorylated forms

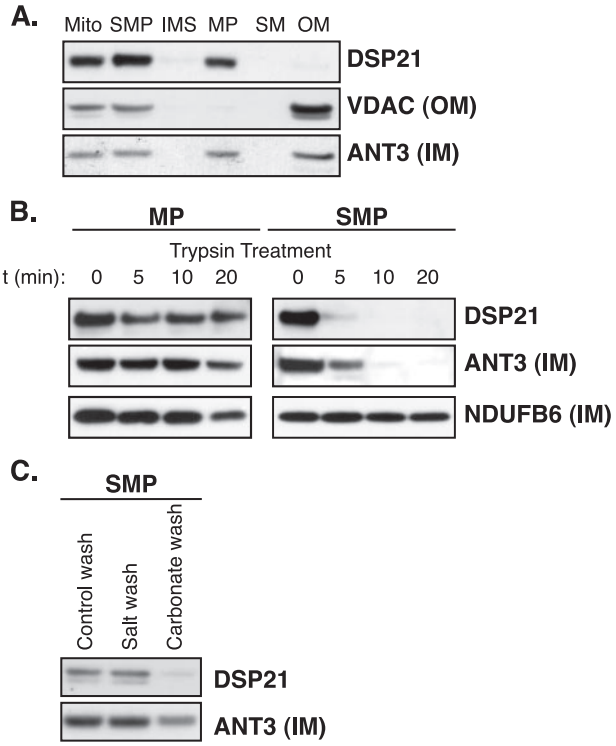

FIGURE 6. **DSP21 is a peripheral mitochondrial inner membrane protein facing the matrix.** *A*, 20 μg of each submitochondrial fraction (Fig. 4*A*) were separated by SDS-PAGE and immunoblotted with markers for OM (anti-VDAC), and IM (anti-ANT). *B*, 200 μg of MP and SMP were treated with 2.5 μg of trypsin in 100 μl of buffer for the indicated amounts of time. Samples were pelleted, washed, separated by SDS-PAGE, and immunoblotted with anti-DSP21 and anti-PTPMT1. The Complex 1 subunit NDUFB6 is not susceptible to trypsin digestion and was used as a loading control. *C*, 100 μg of SMP were washed with either control buffer, high salt (200 mM KCl, 2 mM HEPES, pH 7.2), or high pH (0.1 M Na_2CO_3, pH 11.5) buffer, repelleted, washed, and separated out by SDS-PAGE. Immunoblots were probed with antibodies against DSP21and ANT.

TABLE 1

Comparison of catalytic activity of DSP18 and DSP21 to other dual specific phosphatases utilizing pNPP

	K_m	k_{cat}	k_{cat}/K_m
	mM	s^{-1}	$s^{-1}{}_M{}^{-1}$
DSP18[a]	0.46	0.39	848
DSP21[a]	0.92	0.084	91.5
MKP3/rVH6[b]	9.85	0.16	1.58
PTPMT1[c]	5.9	0.91	153.2
VHR[d]	1.59	5.2	3240

[a] Data are from this study.
[b] Data are from Wiland *et al.* (40).
[c] Data are from Pagliarini *et al.* (41).
[d] Data are from Denu (39).

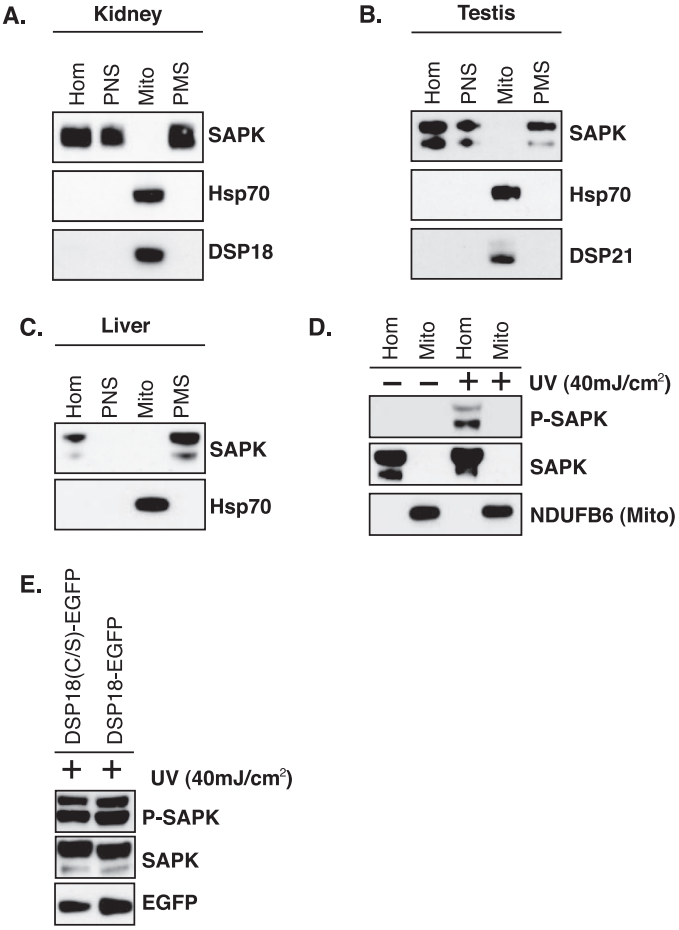

FIGURE 7. **Endogenous SAPK/JNK is not localized to mitochondria.** *A*, rat kidneys were isolated and homogenized (*HOM*), nuclei and unbroken cells were removed (post-nuclear supernatant (PNS)), Mito were removed, and the post-mitochondrial supernatant (*PMS*) was collected. Fractions were separated out by SDS-PAGE and immunoblotted with antibodies against both the p54 and p46 SAPK/JNK isoforms, mitochondrial marker protein Hsp70, and DSP18. *B*, fractions collected from testis tissue were separated out by SDS-PAGE and immunoblotted with antibodies against SAPK/JNK, Hsp70, and DSP21. *C*, fractions collected from rat liver tissue were separated out by SDS-PAGE and immunoblotted with antibodies against SAPK/JNK and Hsp70. *D*, HEK-293A cells were homogenized (*Hom*), and Mito were isolated by differential centrifugation after treatment with 40 mJ/cm^2 of UV radiation and compared with untreated controls. Fractions were separated out and immunoblotted with antibodies against phospho (*p*)-SAPK/JNK (active), SAPK/JNK, and NDUFB6. *E*, HEK-293A cells transfected with DSP18-EGFP or a catalytic inactive mutant DSP18(C/S)-EGFP. After 24 h cells were treated with 40 mJ/cm^2 of UV radiation, and equal amounts of whole cell lysate were separated out by SDS-PAGE and analyzed for changes in SAPK/JNK phosphorylation.

of SAPK/JNK. Phospho-SAPK/JNK was detected in the whole cell lysates of irradiated cells but not in the mitochondria after UV radiation (Fig. 7*D*). Furthermore, we were unable to detect a change in phospho-SAPK/JNK levels in UV-irradiated HEK-293A cells overexpressing DSP18 when compared with a catalytically inactive mutant (Fig. 7*E*).

Collectively these data demonstrate the MAPK SAPK/JNK is not localized to the same subcellular compartment as DSP18 and, therefore, is highly unlikely to be its *in vivo* substrate under physiological conditions. We can rationalize the result obtained by Wu *et al.* (42) on the basis of overexpression of DSP18 leads to inappropriate localization and SAPK/JNK dephosphorylation. This underscores the importance of accurately determining the subcellular localization of substrate and enzyme. However, we should also point out that our observations do not rule out the possibility that under specific signaling conditions SAPK/JNK or DSP18 could be re-directed to a common subcellular compartment where the phosphatase could catalyze SAPK/JNK dephosphorylation.

DSP18 Is Released from the IMS during Apoptosis—Because DSP18 targets to the IM within the IMS compartment, we considered whether DSP18 would be released into the cytosol upon induction of apoptosis, similar to cytochrome *c* (cyt c). Cells treated with the nonspecific kinase inhibitor staurosporine, which induces apoptosis through a BAX- and BAK-mediated

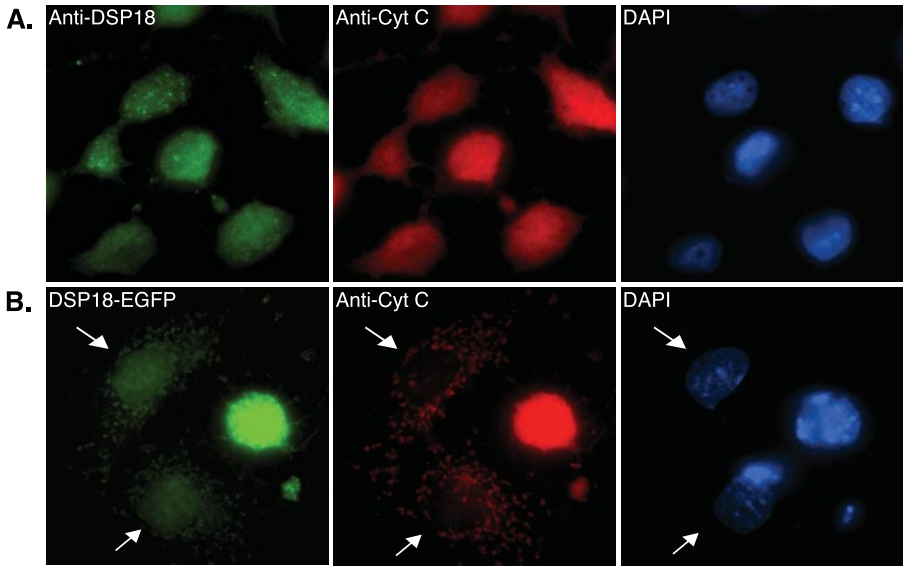

FIGURE 8. **Induction of apoptosis causes translocation of DSP18 from mitochondria into the cytosol.** COS-7 cells stained with anti-DSP18 (*A*) or transfected with DSP18-EGFP (*B*) were chemically induced to undergo apoptosis. Cells were co-stained with anti-cyt c antibody and DAPI, then visualized by IF for release of cyt c from mitochondria into the cytosol. *White arrows* (*B*) indicate a cell not undergoing apoptosis. DAPI staining demonstrates characteristic nuclear condensation and fragmentation.

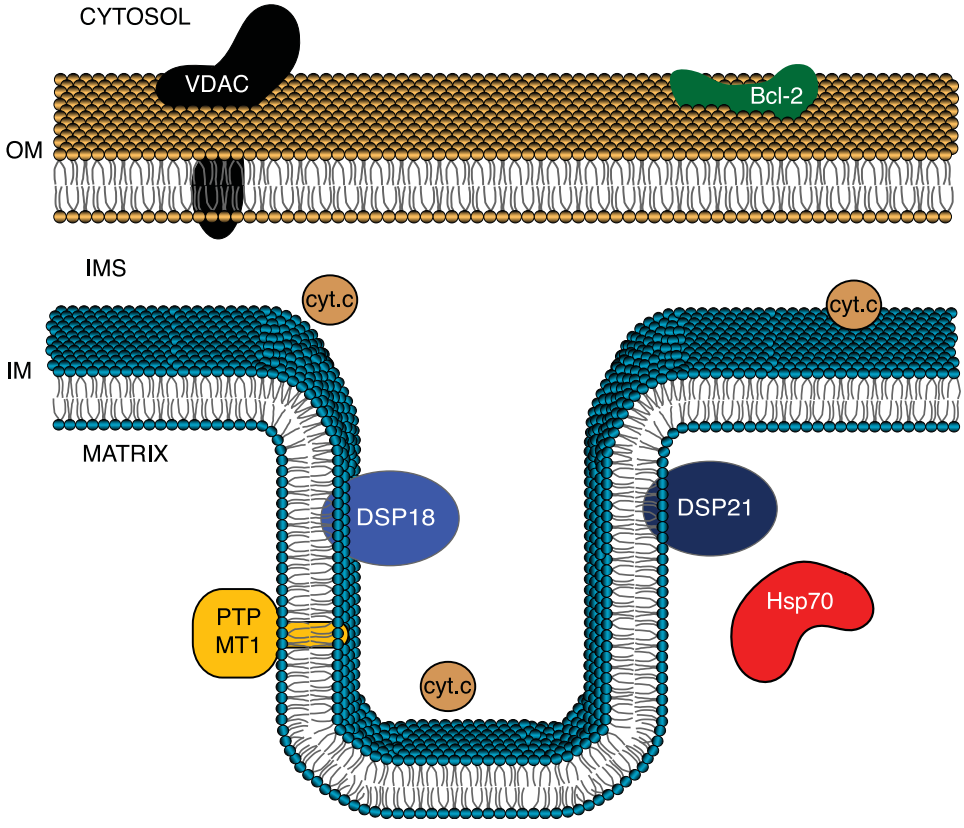

FIGURE 9. **Schematic representation of where the dual specificity phosphatases are localized to in the mitochondria.** *Bcl-2*, B cell lymphoma 2; *PTP-MT1*, protein-tyrosine phosphatase localized to mitochondria 1. Proteins are not drawn to scale.

pathway, results in release of cyt c into the cytosol (44–46). Endogenous DSP18 and cyt c showed cytosolic localization after treatment with staurosporine (Fig. 8*A*). Likewise, cells overexpressing DSP18-EGFP showed cytosolic localization with treatment (Fig. 8*B*). Similar results were observed using the topoisomerase II inhibitor etoposide (data not shown). These results indicate that DSP18 translocates from the IMS compartment to the cytosol upon mitochondrial OM permeabilization during apoptosis.

DISCUSSION

Mitochondria are dynamic organelles that, in addition to their role in bioenergetics, regulate numerous cellular signaling processes ranging from calcium homeostasis to programmed cell death (47–49). Disruption of these key signaling events can increase the risk of age related disorders, cardiovascular disease, neurodegeneration, diabetes, and cancer (48, 50–52). Given its role in multiple cellular processes, reversible phosphorylation will also likely play a significant role in regulating mitochondrial functions. Currently there are more than 60 reports of mitochondrial phosphoproteins as well as ~27 kinases and 10 phosphatases that are reportedly localized to the mitochondrion (10). Many of the kinase and phosphatase localizations have not been rigorously examined. In the present study we have clearly shown for the first time that a dual specificity phosphatase, DSP18, is localized to the IMS compartment of mitochondria. We also identified a highly similar phosphatase, DSP21, as a protein selectively expressed in testes that resides within the mitochondrion. In contrast to DSP18, DSP21 is localized to the matrix compartment of mitochondria. DSP18 and DSP21 are both associated with the IM and can be released after an alkaline wash, making them classical peripheral membrane proteins. Given the similarity between DSP18 and DSP21, it is intriguing that they are located on opposing sides of the IM. Interestingly, this is not the first case of two highly similar proteins being targeted to opposite sides of the IM. The yeast AAA proteases, Yme1 and Yta10 with homologs in humans, are also targeted to the IM but are oriented so they face opposing compartments (53). This places DSP18 and DSP21 in unique locations for

regulating signaling processes within mitochondria via reversible phosphorylation (Fig. 9). Finally, our data suggest that DSP18 is released from the mitochondrial IMS after induction of specific apoptotic signals that result in mitochondrial outer membrane permeabilization.

Previously, published reports claimed that DSP18 and DSP21 are localized to the nucleus and cytoplasm (24, 42). However, these were overexpression experiments utilizing N-terminal tags which have been shown to commonly disrupt the localization of mitochondrial proteins (54). Our data demonstrate that N-terminal tags block the ability of DSP18 and DSP21 to localize to mitochondria either by interfering with the mitochondrial localization signal or translocation machinery. Additionally, previous work demonstrated that recombinant DSP18 and DSP21 exhibits *in vitro* phosphatase activity against MAPK-like phosphopeptides, suggesting that DSP18 may have an *in vivo* preference for phosphorylated tyrosine residues over phosphoserine/threonine residues (24). Although preliminary data from our laboratory support this suggestion, questions still remain regarding a physiological substrate(s). Recent work using an overexpression system has suggested that the MAPK SAPK/JNK is an *in vivo* substrate for DSP18 (42). However, this is in contrast to previously reported data demonstrating no *in vivo* phosphatase activity against a variety of MAPKs including SAPK/JNK (24). Classical MAPK phosphatases contain CH2 and kinase interaction motifs, modules that allow them to recognize their MAPK substrates; however, DSP18 and DSP21 lack these binding motifs, suggesting a unique substrate recognition motif for these phosphatases (22, 24). Furthermore, we were unable to detect any SAPK/JNK localized to the mitochondria, indicating that it is not likely a substrate for DSP18 within the IMS compartment.

We identified a highly conserved internal mitochondrial localization signal in DSP18 and DSP21. Roughly one-third of known mitochondrial proteins do not contain classical N-terminal signal sequences; yet, alternative import signals such as internal mitochondrial localization signal have not been well defined (55, 56). Additionally, many proteins containing an internal mitochondrial localization signal are directed to either the OM, IMS, or IM (55). For example, the IMS protein cyt c and the IM protein ATP/ADP translocase (ANT) both contain an internal mitochondrial localization signal (57). This is consistent with our finding that endogenous DSP18 and DSP21 localize to the IM (Fig. 5). To date, DSP18 is the only DSP shown to localize to the IMS compartment, whereas DSP21 is the second DSP to be found predominantly within the matrix; therefore, they are in distinctive locations for regulating the function of mitochondrial processes by dephosphorylation of proteins both within the IMS and the matrix.

Our data shows that DSP18 is released from the mitochondrial IM of the IMS after induction of apoptotic events. These events result in mitochondrial outer membrane permeabilization and release of apoptogenic factors. Because DSP18 is tightly associated with the IM, its release into the cytosol after OM permeabilization is likely not an artifact. Unlike cyt c, there is precedence for IMS proteins such as apoptosis-inducing factor to require proteolysis to enable release (58). It is possible that such a process is required for DSP18 release. DSP18 is in a unique position to regulate signaling processes after its liberation into the cytosol, or perhaps its release into the cytosol allows for key phosphorylation events to take place in the IMS to potentiate the apoptotic process. Further exploration of the substrate for DSP18 as well as mouse knock-out models should elucidate its role(s) in mitochondrial biology as well as in apoptotic processes.

Thus, DSP18 and DSP21 are in different, but intriguing, mitochondrial compartments to regulate signaling processes. Although few PTPs have well defined *in vivo* substrates, our work, which rigorously determines their location within mitochondria, dramatically narrows the number of potential phosphoprotein substrates. Further exploration of the substrates for DSP18 and DSP21 should elucidate their role(s) in mitochondrial biology.

Acknowledgments—We thank Dr. Gregory S. Taylor for technical assistance with phosphatase assays and helpful discussion, Dr. Marilyn Farquhar and Timo Meerloo for assistance in our immunogold EM experiments, Dr. Amy Carroll for kindly providing the anti-ANT antibodies, Dr. Morton Printz for providing animals, and members of the Dixon laboratory for helpful discussions and critical reading of this manuscript.

REFERENCES

1. Hunter, T. (2000) *Cell* **100,** 113–127
2. Tonks, N. K., and Neel, B. G. (1996) *Cell* **87,** 365–368
3. Alonso, A., Sasin, J., Bottini, N., Friedberg, I., Friedberg, I., Osterman, A., Godzik, A., Hunter, T., Dixon, J., and Mustelin, T. (2004) *Cell* **117,** 699–711
4. Visconti, P. E., and Kopf, G. S. (1998) *Biol. Reprod.* **59,** 1–6
5. Wang, H. G., Rapp, U. R., and Reed, J. C. (1996) *Cell* **87,** 629–638
6. Zha, J., Harada, H., Yang, E., Jockel, J., and Korsmeyer, S. J. (1996) *Cell* **87,** 619–628
7. Linn, T. C., Pettit, F. H., and Reed, L. J. (1969) *Proc. Natl. Acad. Sci. U. S. A.* **62,** 234–241
8. Feliciello, A., Gottesman, M. E., and Avvedimento, E. V. (2005) *Cell. Signal.* **17,** 279–287
9. Horbinski, C., and Chu, C. T. (2005) *Free Radic. Biol. Med.* **38,** 2–11
10. Pagliarini, D. J., and Dixon, J. E. (2006) *Trends Biochem. Sci.* **31,** 26–34
11. Salvi, M., Brunati, A. M., and Toninello, A. (2005) *Free Radic. Biol. Med.* **38,** 1267–1277
12. Valente, E. M., Abou-Sleiman, P. M., Caputo, V., Muqit, M. M., Harvey, K., Gispert, S., Ali, Z., Del Turco, D., Bentivoglio, A. R., Healy, D. G., Albanese, A., Nussbaum, R., Gonzalez-Maldonado, R., Deller, T., Salvi, S., Cortelli, P., Gilks, W. P., Latchman, D. S., Harvey, R. J., Dallapiccola, B., Auburger, G., and Wood, N. W. (2004) *Science* **304,** 1158–1160
13. Holness, M. J., and Sugden, M. C. (2003) *Biochem. Soc. Trans.* **31,** 1143–1151
14. Wynn, R. M., Kato, M., Machius, M., Chuang, J. L., Li, J., Tomchick, D. R., and Chuang, D. T. (2004) *Structure* **12,** 2185–2196
15. Cook, K. G., Lawson, R., and Yeaman, S. J. (1983) *FEBS Lett.* **157,** 59–62
16. Pagliarini, D. J., Wiley, S. E., Kimple, M. E., Dixon, J. R., Kelly, P., Worby, C. A., Casey, P. J., and Dixon, J. E. (2005) *Mol. Cell* **19,** 197–207
17. Rosini, P., De Chiara, G., Bonini, P., Lucibello, M., Marcocci, M. E., Garaci, E., Cozzolino, F., and Torcia, M. (2004) *J. Biol. Chem.* **279,** 14016–14023
18. Salvi, M., Stringaro, A., Brunati, A. M., Agostinelli, E., Arancia, G., Clari, G., and Toninello, A. (2004) *Cell. Mol. Life Sci.* **61,** 2393–2404
19. Cardone, L., Carlucci, A., Affaitati, A., Livigni, A., DeCristofaro, T., Garbi, C., Varrone, S., Ullrich, A., Gottesman, M. E., Avvedimento, E. V., and Feliciello, A. (2004) *Mol. Cell. Biol.* **24,** 4613–4626
20. Cardone, L., de Cristofaro, T., Affaitati, A., Garbi, C., Ginsberg, M. D., Saviano, M., Varrone, S., Rubin, C. S., Gottesman, M. E., Avvedimento,

E. V., and Feliciello, A. (2002) *J. Mol. Biol.* **320,** 663–675
21. Livigni, A., Scorziello, A., Agnese, S., Adornetto, A., Carlucci, A., Garbi, C., Castaldo, I., Annunziato, L., Avvedimento, E. V., and Feliciello, A. (2006) *Mol. Biol. Cell* **17,** 263–271
22. Alonso, A., Rojas, A., Godzik, A., and Mustelin, T. (2004) *Top. Curr. Genet.* **5,** 333–358
23. Barford, D., Das, A. K., and Egloff, M. P. (1998) *Annu. Rev. Biophys. Biomol. Struct.* **27,** 133–164
24. Hood, K. L., Tobin, J. F., and Yoon, C. (2002) *Biochem. Biophys. Res. Commun.* **298,** 545–551
25. Wu, Q., Gu, S., Dai, J., Dai, J., Wang, L., Li, Y., Zeng, L., Xu, J., Ye, X., Zhao, W., Ji, C., Xie, Y., and Mao, Y. (2003) *Biochim. Biophys. Acta* **1625,** 296–304
26. Jeong, D. G., Cho, Y. H., Yoon, T. S., Kim, J. H., Son, J. H., Ryu, S. E., and Kim, S. J. (2006) *Acta Crystallogr. D Biol. Crystallogr.* **62,** 582–588
27. Lennon, G., Auffray, C., Polymeropoulos, M., and Soares, M. B. (1996) *Genomics* **33,** 151–152
28. Taylor, G. S., and Dixon, J. E. (2003) *Methods Enzymol.* **366,** 43–56
29. Kim, S. A., Taylor, G. S., Torgersen, K. M., and Dixon, J. E. (2002) *J. Biol. Chem.* **277,** 4526–4531
30. Taylor, G. S., Liu, Y., Baskerville, C., and Charbonneau, H. (1997) *J. Biol. Chem.* **272,** 24054–24063
31. Lapidus, R. G., and Sokolove, P. M. (1993) *Arch. Biochem. Biophys.* **306,** 246–253
32. Piergiacomi, V. A., Palacios, A., and Catala, A. (1996) *Mol. Cell. Biochem.* **165,** 121–125
33. Johnson, D., and Lardy, H. (1967) *Methods Enzymol.* **10,** 94–96
34. Liou, W., Geuze, H. J., and Slot, J. W. (1996) *Histochem. Cell Biol.* **106,** 41–58
35. Tokuyasu, K. T. (1980) *Histochem. J.* **12,** 381–403
36. Pedersen, P. L., and Hullihen, J. (1978) *J. Biol. Chem.* **253,** 2176–2183
37. Bossy-Wetzel, E., and Green, D. R. (2000) *Methods Enzymol.* **322,** 235–242
38. Alonso, A., Burkhalter, S., Sasin, J., Tautz, L., Bogetz, J., Huynh, H., Bremer, M. C., Holsinger, L. J., Godzik, A., and Mustelin, T. (2004) *J. Biol. Chem.* **279,** 35768–35774
39. Denu, J. M., Zhou, G., Wu, L., Zhao, R., Yuvaniyama, J., Saper, M. A., and Dixon, J. E. (1995) *J. Biol. Chem.* **270,** 3796–3803
40. Wiland, A. M., Denu, J. M., Mourey, R. J., and Dixon, J. E. (1996) *J. Biol. Chem.* **271,** 33486–33492
41. Pagliarini, D. J., Worby, C. A., and Dixon, J. E. (2004) *J. Biol. Chem.* **279,** 38590–38596
42. Wu, Q., Huang, S., Sun, Y., Gu, S., Lu, F., Dai, J., Yin, G., Sun, L., Zheng, D., Dou, C., Feng, C., Ji, C., Xie, Y., and Mao, Y. (2006) *Front. Biosci.* **11,** 2714–2724
43. Davis, R. J. (2000) *Cell* **103,** 239–252
44. Goldstein, J. C., Waterhouse, N. J., Juin, P., Evan, G. I., and Green, D. R. (2000) *Nat. Cell Biol.* **2,** 156–162
45. Couldwell, W. T., Hinton, D. R., He, S., Chen, T. C., Sebat, I., Weiss, M. H., and Law, R. E. (1994) *FEBS Lett.* **345,** 43–46
46. Wei, M. C., Zong, W. X., Cheng, E. H., Lindsten, T., Panoutsakopoulou, V., Ross, A. J., Roth, K. A., MacGregor, G. R., Thompson, C. B., and Korsmeyer, S. J. (2001) *Science* **292,** 727–730
47. Brookes, P. S., Yoon, Y., Robotham, J. L., Anders, M. W., and Sheu, S. S. (2004) *Am. J. Physiol. Cell Physiol.* **287,** 817–833
48. Duchen, M. R. (2004) *Mol. Aspects Med.* **25,** 365–451
49. Green, D. R. (2005) *Cell* **121,** 671–674
50. Marin-Garcia, J., and Goldenthal, M. J. (2004) *J. Mol. Med.* **82,** 565–578
51. Melov, S. (2004) *Trends Neurosci.* **27,** 601–606
52. Wallace, D. C. (2005) *Annu. Rev. Genet.* **39,** 359–407
53. Koppen, M., and Langer, T. (2007) *Crit. Rev. Biochem. Mol. Biol.* **42,** 221–242
54. Mehrle, A., Rosenfelder, H., Schupp, I., del Val, C., Arlt, D., Hahne, F., Bechtel, S., Simpson, J., Hofmann, O., Hide, W., Glatting, K. H., Huber, W., Pepperkok, R., Poustka, A., and Wiemann, S. (2006) *Nucleic Acids Res.* **34,** 415–418
55. Truscott, K. N., Brandner, K., and Pfanner, N. (2003) *Curr. Biol.* **13,** 326–337
56. Diekert, K., Kispal, G., Guiard, B., and Lill, R. (1999) *Proc. Natl. Acad. Sci. U. S. A.* **96,** 11752–11757
57. Neupert, W. (1997) *Annu. Rev. Biochem.* **66,** 863–917
58. Polster, B. M., Basanez, G., Etxebarria, A., Hardwick, J. M., and Nicholls, D. G. (2005) *J. Biol. Chem.* **280,** 6447–6454